

# Explicitly Accounting for Pixel Dimension in Calculating Classical and Fractal Landscape Shape Metrics

Attila R. Imre · Duccio Rocchini

Received: 5 June 2008 / Accepted: 12 January 2009 / Published online: 29 January 2009  
© Springer Science+Business Media B.V. 2009

**Abstract** Different summarized shape indices, like mean shape index (MSI) and area weighted mean shape index (AWMSI) can change over multiple size scales. This variation is important to describe scale heterogeneity of landscapes, but the exact mathematical form of the dependence is rarely known. In this paper, the use of fractal geometry (by the perimeter and area Hausdorff dimensions) made us able to describe the scale dependence of these indices. Moreover, we showed how fractal dimensions can be deducted from existing MSI and AWMSI data. In this way, the equality of a multiscale tabulated MSI and AWMSI dataset and two scale-invariant fractal dimensions has been demonstrated.

**Keywords** AWMSI · Fractal dimension · Landscape metrics · Landscape pattern · MSI · Shape index

## 1 Introduction

### 1.1 Measuring Shape in Landscape Ecology

Shape of spatial entities, habitats and ecosystems represents a key information for landscape ecologists since it carries key information on landscape structure and potentially on processes which may have generated it (O'Neill et al. 1988).

In most cases, land cover maps are used for ascertain landscape shape complexity and they are composed by vector- or pixel-entities. Such entities represent landscape

---

A. R. Imre (✉)

KFKI Atomic Energy Research Institute, P.O. Box 49, 1525 Budapest, Hungary  
e-mail: imre@aeki.kfki.hu

D. Rocchini

TerraData environmetrics, Dipartimento di Scienze Ambientali “G. Sarfatti”,  
Università di Siena, via P.A. Mattioli 4, 53100 Siena, Italy

patches, once they have been aggregated on the strength of a common attribute like a common land cover class. In this paper we will focus on pixel-based patches, i.e. aggregations of neighbour pixels sharing the same land cover class. This choice has been made since a pixel represents the most cost-effective entity to deal with particularly when maps are directly derived from airborne imagery (Cracknell 1998). In fact, using pixels no additional digitisation or image segmentation procedures are required and semi-automated classification is allowed (Laba et al. 2008). Unfortunately, pixels represent a ‘snare and a delusion’ according to Fisher (1997). In fact they may hide information relative to sub-pixel heterogeneity.

However, in some cases, pixels could represent a straightforward manner for taking into account the spatial resolution of the considered map, just considering pixel size as the minimum mapping unit (like canopy-size for aerial forest photos). It is worth remembering that scale may dramatically impact the achieved results during landscape analysis. Indeed, results of the analyses for the same area can vary because of the spatial resolution (Johnson and Howarth 1987), and some patterns or processes can be recognized only at specific resolutions (Jelinski and Wu 1996). This is particularly true for shape based metrics (Rocchini et al. 2006).

## 1.2 Measures of Shape Using Pixels: Hidden Problems on Spatial Scale

Patch shapes cannot be measured directly, but several indices can be defined to describe shape-related behaviours, like compactness, shape index (SI), interior-to-edge ratio, mean shape index (MSI), area weighted mean shape index (AWMSI), several kinds of fractal dimensions (Hausdorff, Minkowski, etc.) and various entropies. Some of these indices are resolution-independent, some of them are not. For the ones with resolution-dependence (i.e. values depending on the actual pixel size) the forms of the dependencies are rarely known (see for example DiBari 2003; Rocchini 2005; Uuemaa et al. 2005; Carranza et al. 2007). In this short paper, we are going to derive the pixel-size dependence for MSI and AWMSI for patches which can be approximated as fractals.

The mostly used landscape shape metrics are based on perimeter/area ratio (Wu et al. 2000b; Bogaert et al. 2002; Moser et al. 2002; Uuemaa et al. 2005; Frohn and Hao 2006; Heegaard et al. 2007; Saura and Castro 2007) such as (for raster datasets):

$$SI = \frac{0.25P_i}{\sqrt{A_i}} \quad (1)$$

where SI is the shape index of patch  $i$ . SI directly estimates individual shape complexity (also called compactness). The minimum value is around 0.89, related to the circle.

Obviously considering a set of  $N$  patches composing a class within a landscape or a whole landscape as well, the mean of all SIs (MSI) or the mean weighted on occupied area (AWMSI) is simply extracted as:

$$MSI = \frac{\sum_{i=1}^N \frac{0.25P_i}{\sqrt{A_i}}}{N} \quad (2)$$

$$AWMSI = \sum_{i=1}^N \left( \frac{0.25P_i}{\sqrt{A_i}} \right) \left( \frac{A_i}{\sum_{j=1}^N A_j} \right). \tag{3}$$

Unfortunately, the relation between such measures and pixel dimension have been poorly modelled (see e.g. Wu et al. 2000a) and no explicit reference to pixel size is made in their mathematical solution. General relations cannot be constructed, but in special cases—when the patches can be approximated as fractals—one can deduct a relation describing the resolution-dependence of the shape indices.

## 2 Methods

### 2.1 Solution Using Hausdorff Dimension and Spatial Indices

Fractals are statistically self-similar mathematical objects (Mandelbrot 1982), i.e. most of their shape-related properties are scale-invariant. It means that while Euclidean length and area can depend on the resolution, their fractal counterparts are resolution-independent; all size-dependences are included into the fractal dimension. In reality, a patch can be handled as fractal only in a limited size range. In landscape metric, the lower limit cannot be below the natural units of the landscape (for example in a forest-patch, the natural unit is a tree), while the higher limit cannot be bigger than the characteristic linear size (like maximal diameter) of the patch. Fractals have been used to help to describe landscapes since the “foundation” of fractal geometry (Mandelbrot 1982) with more or less success. Unfortunately sometimes fractal geometry is handled as a miraculous panacea, which can solve all problems; it is not true, it can be used only with serious limitations. But after defining those limitations, it is really a useful tool for example to simplify spatial indices (Burrough 1981; Mandelbrot 1982; Krummel et al. 1987; Milne 1988; Sugihara and May 1990; LaGro 1991; Olsen et al. 1993; Li 2000; Imre and Bogaert 2004, 2006). There are several, deeply different fractal dimensions, i.e. Hausdorff, box, Minkowski, Korcak, etc. (Mandelbrot 1982; Feder 1988; Russ 1994). The one most often referred as “fractal dimension” is the Hausdorff dimension, also used in our description.

One can measure perimeter length and area of a patch on variable scale as:

$$A(L) = C_A L^{D_A} \tag{4}$$

$$P(L) = C_P L^{D_P} \tag{5}$$

where  $L$  is some characteristic linear size (for example maximal diameter),  $D_s$  are the corresponding fractal (Hausdorff) dimensions and  $C_s$  are the corresponding form-factors (for circles,  $C_P = \pi$  and  $C_A = \pi/4$ , when  $L$  is the diameter). In Euclidean geometry,  $D_P = 1$  and  $D_A = 2$ ; thus when having a circle, the perimeter will scale as  $L^1$  while area will scale with  $L^2$ .

As it can be seen on Eqs. 1–3, all indices (SI, MSI and AWMSI) depends on  $P/A^{-1/2}$ , therefore when one wants to calculate the influence of fractal dimension on these indices, this quotient should be calculated first. In these calculation, similarity

of the patches will be expected, i.e. all patches should have the same fractal dimensions and form factors. It is strong criterion but it is required in all multi-patch fractal analysis and in many cases it is satisfied (Imre and Bogaert 2004).

For regular formations (regular means that for example all of them will be square-shaped or circular, etc.), the perimeter dimensions will be 1 and area dimensions 2, therefore for the  $i$ th patch:

$$\frac{P_i}{\sqrt{A_i}} = \frac{C_{P_i}}{\sqrt{C_{A_i}}} \tag{6}$$

This is a very rare case, usually a forest patch can be seen as an object with almost Euclidean area but with rugged perimeter. This means that by increasing the resolution, the area will change only with a small amount, while the perimeter might change drastically, as smaller and smaller irregularities reveal themselves. Therefore for islands, forest patches, etc., researchers usually assume that  $D_{A_i}$  is 2 for each spot while  $D_{P_i} = 1 + \delta$ , where  $\delta$  is a small positive number (same for each spot), a criterion widely used in the so-called perimeter-area method (see for example Mandelbrot et al. 1984; Imre 1992, 2006; Russ 1994; Zurlini et al. 2006).

In this case:

$$\frac{P_i}{\sqrt{A_i}} = \frac{C_{P_i}}{\sqrt{C_{A_i}}} L_i^\delta \tag{7}$$

The most probable case occurs when  $D_{P_i} = 1 + \delta$  and  $D_{A_i} = 2 - \alpha$ , i.e. both the perimeter and area are fractals. In that case:

$$\frac{P_i}{\sqrt{A_i}} = \frac{C_{P_i}}{\sqrt{C_{A_i}}} L_i^{\delta + \frac{\alpha}{2}} \tag{8}$$

Eq. 8 can be re-written with the fractal dimensions, as:

$$\frac{P_i}{\sqrt{A_i}} = \frac{C_{P_i} L_i^{D_{P_i}}}{\sqrt{C_{A_i} L_i^{D_{A_i}/2}}} = \frac{C_{P_i}}{\sqrt{C_{A_i}}} L_i^{(D_{P_i} - \frac{D_{A_i}}{2})} \tag{9}$$

Eqs. 8 and 9 are equivalent.

After deducting  $P/A^{-1/2}$ , we can calculate the fractal dimension dependencies of the SI, MSI and AWMSI indices. For SI (which is an index for individual patches) the only requirement is the fractality, while for MSI and AWMSI all individual islands have to be fractal plus their fractal dimensions and form-factors have to be nearly the same, i.e. they have to be statistically similar. When a set of patches is generated by the same physical, chemical, biological, etc. process, this requirement is very often satisfied (Mandelbrot 1982; Vicsek 1989).

Using these fractal and similarity approximations, SI for each separate patch can be written as:

$$SI_i = \frac{0.25 C_{P_i}}{\sqrt{C_{A_i}}} L_i^{\delta + \frac{\alpha}{2}} \tag{10}$$

For MSI and AWMSI, one more step is necessary, due to the summarization. Studying the  $i$ th patch with different resolution (where  $\varepsilon$  is the pixel-size), the characteristic

linear size will be proportional with  $1/\varepsilon$  (doubling the pixel size, the diameter will be the half, given in pixels), therefore we can separate each  $L_i$  into two different part:

$$L_i = \frac{1}{\varepsilon} u(i) \tag{11}$$

where  $\varepsilon$  is the resolution. In this way,  $L$  depends on the resolution and also has a not necessarily analytical dependence on  $i$  (island index) by  $u(i)$ . The proportionality factor between the resolution and characteristic linear size can be included into  $u$ . Now MSI and AWMSI for a set of patches (where  $N$  is the total number of patches) can be written as:

$$MSI = \frac{\sum_{i=1}^N \frac{0.25P_i}{\sqrt{A_i}}}{N} = \frac{\sum_{i=1}^N \frac{0.25C_{P_i}}{\sqrt{C_{A_i}}} L_i^{\delta+\frac{\alpha}{2}}}{N} = \left( \sum_{i=1}^N \frac{0.25C_{P_i}}{N\sqrt{C_{A_i}}} u(i)^{\delta+\frac{\alpha}{2}} \right) \left( \frac{1}{\varepsilon} \right)^{\delta+\frac{\alpha}{2}} \tag{12}$$

$$\begin{aligned} AWMSI &= \sum_{p=1}^N \left( \frac{0.25P_i A_i}{\sqrt{A_i} \sum_{j=1}^N A_j} \right) = \sum_{i=1}^N \frac{0.25C_{P_i} \sqrt{C_{A_i}} L_i^{D_{P_i}+D_{A_i}/2}}{\sum_{j=1}^N C_{A_j} L_j^{D_{A_p}}} \\ &= \left( \sum_{i=1}^N \frac{0.25C_{P_i} \sqrt{C_{A_i}} u(i)^{2+\delta+\alpha/2}}{\sum_{j=1}^N C_{A_j} u(j)^{2-\alpha}} \right) \left( \frac{1}{\varepsilon} \right)^{\delta+\frac{3\alpha}{2}} \end{aligned} \tag{13}$$

In this way, the size-dependence of these indices could be obtained. In a simplified form, keeping only the resolution-dependence, MSI and AWMSI can be written as:

$$MSI(\varepsilon) = \text{const}(MSI) \left( \frac{1}{\varepsilon} \right)^{\delta+\frac{\alpha}{2}} \tag{14}$$

$$AWMSI(\varepsilon) = \text{const}(AWMSI) \left( \frac{1}{\varepsilon} \right)^{\delta+\frac{3\alpha}{2}} \tag{15}$$

where all  $\varepsilon$ -independent parts are included into the constants.

In the following section we are going to analyse MSI and AWMSI of a few landscape structures to demonstrate the usability of this fractal description and to obtain information about the geometry of these structures. SI will not be considered separately in this paper since both MSI and AWMSI directly derived from SI. Thus, analysing even SI would bring little information in our case and could only create some confusion about the hypothesis being tested.

### 3 Results and Discussion

#### 3.1 Application to Landscape Structures

In this section, the previously deducted results have been applied for a set of landscape structures. These structures are located in a 440-hectare part of the Natural Reserve of Poggio all’Olmo on the slope of Mt. Amiata (longitude  $11^{\circ}32'26''E$ , latitude  $42^{\circ}58'36''$ , datum WGS84), Italy. An aerial photograph was taken from 6,000 m and scanned at a 600 dpi resolution. Further details of the area

and the complete classical data analysis (SI, MSI, AWMSI, etc.) can be found elsewhere (see Rocchini 2005; Rocchini et al. 2006). Seven different land cover classes were separated in the original study (Fig. 1): (1) woodlands, i.e. *Quercus cerris* woodlands, mixed broad-leaf woodlands (dominated by *Quercus pubescens*, *Ostrya carpinifolia* and *Quercus cerris*), riparian woody vegetation (dominated by *Populus nigra*, *Ulmus minor*, *Acer campestre*, *Tilia platyphyllos* and *Ostrya carpinifolia* or *Salix* sp.pl.), maple thickets and chestnut woodlands; (2) shrublands, i.e. *Prunus spinosa* and *Cytisus scoparius* shrublands; (3) open formations, i.e. semi-natural grasslands (*Bromus erectus* grasslands and *Arrhenatherum elatius* grasslands) and small cultivated fields; (4) buildings, i.e. small rural houses; (5) isolated or grouped trees, (6) linear formations, i.e. hedges; (7) coniferous plantations, i.e. exotic conifers (*Abies alba*, *Cupressus arizonica*, *Pinus nigra*, *Pinus sylvestris*, *Pseudotsuga menziesii*) which do not reproduce spontaneously, planted in the 1950–1970s. We refer to Angiolini et al. (1999), Maccherini et al. (2001) or Rocchini et al. (2006) for a complete description of the vegetation of the area.

Operationally speaking, the previously described classes were attributed following an inner dominance criterion, within each cell. In practice, the aerial photograph was sub-sampled by superimposing a grid with a variable cell dimension (10, 20 and 40 m). Each cell was semi-automatically classified in order to simulate photo-interpretation at different resolutions. The classification process required a manual classification, i.e. a visual attribution based on the aerial photograph, of each grid cell at 10 m spatial resolution. The semi-automatic classification involved strata with 20 and 40 m spatial resolutions. Where cells of

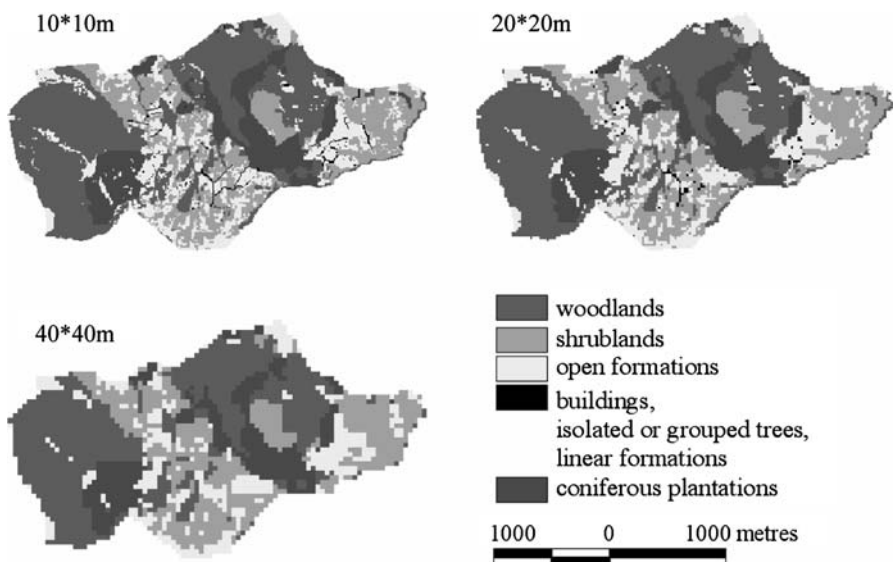


**Fig. 1** Land cover map of the Natural Reserve of Poggio all'Olmo, Italy, at different spatial resolutions:  $10 \times 10$ ,  $20 \times 20$ ,  $40 \times 40$  m. Notice that buildings, isolated or grouped trees and linear formations were all represented by a black colour. In fact, they cannot be seen at a resolution of  $40 \times 40$  m. Thus they were removed from the analysis

**Table 1** MSI of each land cover class at different spatial resolutions (further details in the text)

	10 × 10 m	20 × 20 m	40 × 40 m
Woodlands	1.67	1.69	1.57
Shrublands	1.62	1.65	1.74
Open formations	1.44	1.40	1.32
Coniferous plantations	1.91	1.73	1.65

**Table 2** AWMSI of each land cover class at different spatial resolutions (further details in the text)

	10 × 10 m	20 × 20 m	40 × 40 m
Woodlands	3.4	2.7	2.5
Shrublands	5.8	4.6	3.6
Open formations	3.6	2.7	1.8
Coniferous plantations	3.0	2.5	2.7

larger cell dimension were completely dominated by a single class at the 10 m level, they were automatically attributed to that class at the 20 and/or 40 m level. Otherwise, they were manually re-classified at the 20 and/or 40 m level.

MSI and AWMSI values were determined for the rasterized map with the pixel-size of 10 × 10, 20 × 20 and 40 × 40 m (see Tables 1, 2) by Rocchini (2005). Buildings, isolated or grouped trees and linear formations cannot be seen with 40 × 40 m pixel-size, since these objects are less than 40 × 40 m in size (Rocchini 2005) therefore only the four other groups were analyzed.

On Figs. 2 and 3, double logarithmic plot of linear size  $2(L = 1/\text{pixel size})$  versus MSI and AWMSI can be seen. From Eqs. 14 and 15, the double logarithmic plot should be linear (when the fractality holds):

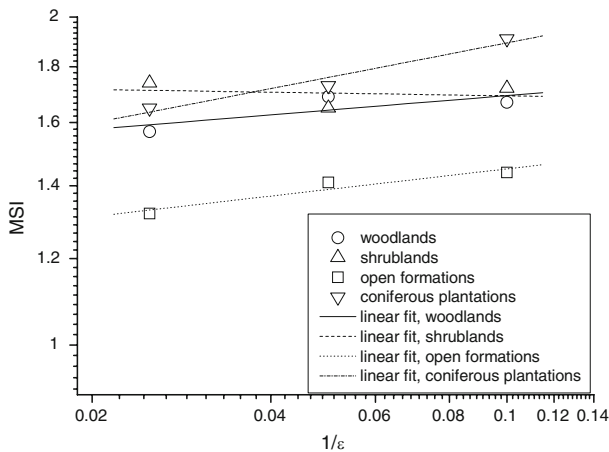


**Fig. 2** The resolution-dependence of the mean shape index in different land-cover classes

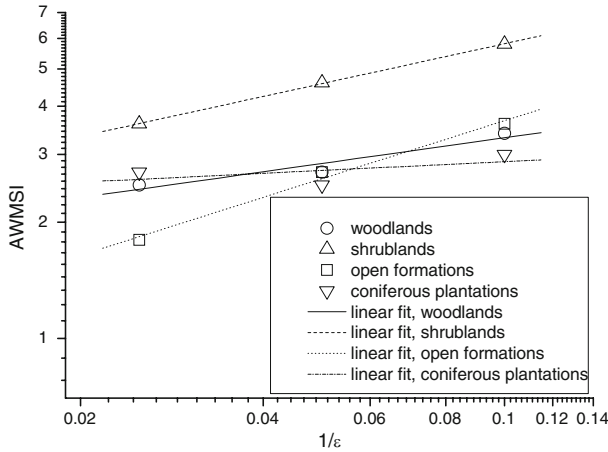


**Fig. 3** The resolution-dependence of the area-weighted mean shape index in different land-cover classes

$$\log \text{MSI} = \log[\text{const}(\text{MSI})] + \left(\delta + \frac{\alpha}{2}\right)L = A + BL \tag{16}$$

$$\log \text{AWMSI} = \log[\text{const}(\text{AWMSI})] + \left(\delta + \frac{3\alpha}{2}\right)L = C + DL \tag{17}$$

where  $A = \log[\text{const}(\text{MSI})]$ ,  $B = (\delta + \alpha/2)$ ,  $C = \log[\text{const}(\text{AWMSI})]$  and  $D = (\delta + 3\alpha/2)$ .  $A$ ,  $B$ ,  $C$  and  $D$  constants are reported in Table 3. The fractal increments can be calculated from  $B$  and  $D$ :

$$\alpha = D - B \tag{18}$$

$$\delta = \frac{3B - D}{2} \tag{19}$$

These increments and the corresponding fractal dimensions (together with their error) are also reported in Table 3.

Some major issues are related to the application of fractal description of land cover objects. First of all, it can be applied only with some errors (see Figs. 2, 3; Table 3). Theoretically  $\alpha$  and  $\delta$  can change between 0 and 1 (being in two dimension  $1 \leq D_P \leq 2$  and  $1 \leq D_A \leq 2$ ), therefore the errors (from 0.04 to 0.11) represent 4–11% of the full scale. Another problem is the very limited resolution-range (10–40 m); for a good fractal analysis, two orders of magnitude would be much better (Avnir et al. 1998), but data at a high range in spatial resolutions are usually hard to be obtained, especially when the studied landscape is very fragmented. Therefore—besides demonstrating the applicability of our method—our limited data also can provide useful information.

While for natural woodlands  $D_P = 1.17 \pm 0.09$  and  $D_A = 1.82 \pm 0.07$ , artificial coniferous plantations showed a  $D_P = 1.21 \pm 0.09$  and a  $D_A = 2.03 \pm 0.11$ , the higher than 2 value being caused by the experimental error (practically it means  $D_A = 2$  with some experimental error). Notice the similarity of  $D_P$  in the two cases.

**Table 3** MSI, AWMSI, fractal increments and fractal dimensions for different land cover classes (further details in the text)

	MSI		AWMSI		Fractal increments		Fractal dimensions	
	A	B	C	D	$\alpha$	$\delta$	$D_A$	$D_P$
Woodlands	$0.27 \pm 0.05$	$0.04 \pm 0.04$	$0.74 \pm 0.08$	$0.22 \pm 0.06$	$0.18 \pm 0.07$	$0.17 \pm 0.09$	$1.82 \pm 0.07$	$1.17 \pm 0.09$
Shrublands	$0.22 \pm 0.01$	$-0.01 \pm 0.04$	$1.11 \pm 0.01$	$0.34 \pm 0.01$	$0.34 \pm 0.04$	$0.16 \pm 0.09$	$1.66 \pm 0.04$	$1.16 \pm 0.09$
Open formations	$0.22 \pm 0.02$	$0.06 \pm 0.02$	$1.06 \pm 0.06$	$0.50 \pm 0.05$	$0.44 \pm 0.05$	$0.34 \pm 0.06$	$1.56 \pm 0.05$	$1.34 \pm 0.06$
Coniferous plantations	$0.38 \pm 0.03$	$0.11 \pm 0.02$	$0.53 \pm 0.14$	$0.08 \pm 0.11$	$-0.03 \pm 0.11$	$0.21 \pm 0.09$	$2.03 \pm 0.11$	$1.21 \pm 0.09$

This is related to two main points: (1) a high degree of shape homogeneity of natural woodlands and (2) the unexpected shape complexity of coniferous plantation. Considering the first point, this phenomenon is related to the ecological dynamics of the study area which are in line with previous studies about natural woodland encroachment against seminatural Mediterranean grasslands (see e.g. Romero-Calcerrada and Perry 2004). In fact, after the abandonment of cultural practices including both cultivation and grazing, ligneous species spread. After a first phase of landscape entropy increase caused by shrubland nucleus encroachment, the whole dynamic generally leads to the formation of homogenous highly-sized woodland patches (Rocchini et al. 2006; Millington et al. 2007; Marignani et al. 2008).

Considering the coniferous plantations, the almost exactly two area dimension means a continuous form (no open areas, houses, etc. inside of the plantation). The relatively high perimeter dimension is a little bit unexpected; one would expect that a plantation has smooth perimeter; at least the ruggedness would not be expected in the 10–40 m range. This should be related to the topographic roughness of the Reserve (elevation ranging from 664 to 1,016 m within a 440 ha space) constraining plantations to follow topographic variability, thus being more complex in shape. For comparison, in a fractal study on some pine forests on a relatively flat (barren sandy soils and heatlands), re-forested area (Imre and Bogaert 2004), the average perimeter dimensions were  $1.09 \pm 0.04$ , while the area dimensions were  $1.79 \pm 0.05$  (with 10 m resolution up to a maximum 600 m resolution), compared to the values obtained in this study;  $D_P = 1.21 \pm 0.09$  and  $D_A = 2.03 \pm 0.11$  and  $D_P = 1.17 \pm 0.09$  and  $D_A = 1.82 \pm 0.07$  (with 10–40 m resolution) for re-forested and natural woodlands, respectively.

For shrublands,  $D_P = 1.16 \pm 0.09$  and  $D_A = 1.66 \pm 0.04$ . The low area dimension suggests that the shrublands are not continuous, other formations like clearings and seminatural grasslands are located therein (see even Fig. 1). For the open formations (i.e. seminatural grasslands)  $D_P = 1.34 \pm 0.06$  and  $D_A = 1.56 \pm 0.04$ , suggesting very rugged perimeters and a lot of discontinuity inside. In fact, seminatural grasslands underwent a high fragmentation due to the previously described abandonment of the cultural practices with a shrub and woodland encroached ecological dynamic leading to small isolated grassland patches (Rocchini et al. 2006).

#### 4 Conclusion

The variation of the different summarized shape indices (MSI and AWMSI) over multiple scales is very important for the identification of scale heterogeneity of the landscape. To give a mathematical description of this scale-dependence, we used fractal geometry. It has been concluded that perimeter and area Hausdorff dimensions can be used to describe the scale variance of MSI and AWMSI. Applying our results on a dataset for a 440 ha natural reserve (Natural Reserve of Poggio all'Olmo, Italy) we demonstrated that the fractal dimensions can be deduced from existing MSI and AWMSI data. The obtained fractal dimensions—just like MSI and AWMSI data tabulated in different resolutions—enabled us to

make inference on the ecological status of the different land cover classes (woodlands, shrublands, open formations and coniferous plantations) of the Reserve. In this way, the equality of a multiscale tabulated MSI and AWMSI dataset and two scale-invariant fractal dimensions has been demonstrated, giving the possibility to compare other sets of existing MSI, AWMSI and fractal dimension data.

## References

- Angiolini C, Maccherini S, Chiarucci A, Gabellini A, De Dominicis V (1999) Memoria illustrativa alla carta della vegetazione della Riserva Naturale "Poggio all'Olmo" (Grosseto, Toscana Meridionale). *Atti Mus Stor Nat Maremma* 19:29–47
- Avnir D, Biham O, Lidar D, Malcai O (1998) Is the geometry of nature fractal? *Science* 279:39–40. doi: [10.1126/science.279.5347.39](https://doi.org/10.1126/science.279.5347.39)
- Bogaert J, Myneni RB, Knyazikhin Y (2002) A mathematical comment on the formulae for the aggregation index and the shape index. *Landsc Ecol* 17:87–90. doi: [10.1023/A:1015204923187](https://doi.org/10.1023/A:1015204923187)
- Burrough PA (1981) Fractal dimensions of landscapes and other environmental data. *Nature* 294:240–242. doi: [10.1038/294240a0](https://doi.org/10.1038/294240a0)
- Carranza ML, Acosta A, Ricotta C (2007) Analyzing landscape diversity in time: the use of Rényi's generalized entropy function. *Ecol Indic* 7:505–510. doi: [10.1016/j.ecolind.2006.05.005](https://doi.org/10.1016/j.ecolind.2006.05.005)
- Cracknell AP (1998) Synergy in remote sensing: what's in a pixel? *Int J Remote Sens* 19:2025–2047. doi: [10.1080/014311698214848](https://doi.org/10.1080/014311698214848)
- DiBari JN (2003) Scaling exponent and rank-size distributions as indicators of landscape character and change. *Ecol Indic* 3:275–284. doi: [10.1016/j.ecolind.2003.11.006](https://doi.org/10.1016/j.ecolind.2003.11.006)
- Feder J (1988) *Fractals*. Plenum Press, New York
- Fisher P (1997) The pixel: a snare and a delusion. *Int J Remote Sens* 18:679–685. doi: [10.1080/014311697219015](https://doi.org/10.1080/014311697219015)
- Frohn RC, Hao Y (2006) Landscape metric performance in analyzing two decades of deforestation in the Amazon Basin of Rondonia, Brazil. *Remote Sens Environ* 100:237–251. doi: [10.1016/j.rse.2005.10.026](https://doi.org/10.1016/j.rse.2005.10.026)
- Heegaard E, Okland H, Bratli H, Dramstad E, Engan G, Pedersen O, Solstad H (2007) Regularity of species richness relationships to patch size and shape. *Ecography* 30:589–597
- Imre A (1992) Problems of measuring the fractal dimension by the slit-island method. *Scr Metall* 27: 1713–1716. doi: [10.1016/0956-716X\(92\)90007-2](https://doi.org/10.1016/0956-716X(92)90007-2)
- Imre AR (2006) Artificial fractal dimension obtained by using perimeter-area relationship on digitalized images. *Appl Math Comput* 173:443–449. doi: [10.1016/j.amc.2005.04.042](https://doi.org/10.1016/j.amc.2005.04.042)
- Imre AR, Bogaert J (2004) The fractal dimension as a measure of the quality of habitats. *Acta Biotheor* 52:41–56. doi: [10.1023/B:ACBI.0000015911.56850.0f](https://doi.org/10.1023/B:ACBI.0000015911.56850.0f)
- Imre AR, Bogaert J (2006) The Minkowski–Bouligand dimension and the interior-to-edge ratio of habitats. *Fractals* 14:49–53. doi: [10.1142/S0218348X06003027](https://doi.org/10.1142/S0218348X06003027)
- Jelinski DE, Wu J (1996) The modifiable areal unit problem and implications for landscape ecology. *Landsc Ecol* 11:129–140. doi: [10.1007/BF02447512](https://doi.org/10.1007/BF02447512)
- Johnson DD, Howarth PJ (1987) The effects of spatial resolution on land cover/land use theme extraction from airborne digital data. *Can J Rem Sens* 13:68–75
- Krummel JR, Gardner RH, Sugihara G, O'Neill RV, Coleman PR (1987) Landscape patterns in disturbed environment. *Oikos* 48:321–324. doi: [10.2307/3565520](https://doi.org/10.2307/3565520)
- Laba M, Downs R, Smith S, Welsh S, Neider C, White S, Richmond M, Philpot W, Baveye P (2008) Mapping invasive wetland plants in the Hudson River National Estuarine Research Reserve using quickbird satellite imagery. *Remote Sens Environ* 112:286–300. doi: [10.1016/j.rse.2007.05.003](https://doi.org/10.1016/j.rse.2007.05.003)
- LaGro J Jr (1991) Assessing patch shape in landscape mosaics. *Photogramm Eng Remote Sens* 57:285–293
- Li B-L (2000) Fractal geometry applications in description and analysis of patch patterns and patch dynamics. *Ecol Model* 132:33–50. doi: [10.1016/S0304-3800\(00\)00303-3](https://doi.org/10.1016/S0304-3800(00)00303-3)

- Maccherini S, Chiarucci A, Selvi F, De Dominicis V (2001) Flora vascolare della Riserva Naturale di Poggio all'Olmo (Cinigiano, Grosseto). *Atti Soc Tosc Sci Nat Mem Ser B* 108:27–41
- Mandelbrot BB (1982) *The fractal geometry of Nature*. Freeman, New York
- Mandelbrot BB, Passoja DE, Paullay AJ (1984) Fractal character of fracture surfaces of metals. *Nature* 308:721–722. doi:[10.1038/308721a0](https://doi.org/10.1038/308721a0)
- Marignani M, Rocchini D, Torri D, Chiarucci A, Maccherini S (2008) Planning restoration in a cultural landscape in Italy using an object-based approach and historical analysis. *Landsc Urban Plan* 84:28–37. doi:[10.1016/j.landurbplan.2007.06.005](https://doi.org/10.1016/j.landurbplan.2007.06.005)
- Millington J, Perry G, Romero-Calcerrada R (2007) Regression techniques for examining land use/cover change: a case study of a mediterranean landscape. *Ecosystems (N Y., Print)* 10:562–578. doi:[10.1007/s10021-007-9020-4](https://doi.org/10.1007/s10021-007-9020-4)
- Milne BT (1988) Measuring the fractal geometry of landscapes. *Appl Math Comput* 27:67–79. doi:[10.1016/0096-3003\(88\)90099-9](https://doi.org/10.1016/0096-3003(88)90099-9)
- Moser D, Zechmeister HG, Plutzar C, Sauberer N, Wrška T, Grabherr G (2002) Landscape patch shape complexity as an effective measure for plant species richness in rural landscapes. *Landsc Ecol* 17:657–669. doi:[10.1023/A:1021513729205](https://doi.org/10.1023/A:1021513729205)
- O'Neill RV, Krummel JR, Gardner RH, Sugihara G, Jackson B, DeAngelis DL, Milne BT, Turner MG, Zygmunt B, Christensen SW, Dale VH, Graham RL (1988) Indices of landscape pattern. *Landsc Ecol* 1:153–162. doi:[10.1007/BF00162741](https://doi.org/10.1007/BF00162741)
- Olsen ER, Ramsey RD, Winn DS (1993) A modified fractal dimension as a measure of landscape diversity. *Photogramm Eng Remote Sens* 59:1517–1520
- Rocchini D (2005) Resolution problems in calculating landscape metrics. *J Spat Sci* 50:25–36
- Rocchini D, Perry GLW, Salerno M, Maccherini S, Chiarucci A (2006) Landscape change and the dynamics of open formations in a natural reserve. *Landsc Urban Plan* 77:167–177. doi:[10.1016/j.landurbplan.2005.02.008](https://doi.org/10.1016/j.landurbplan.2005.02.008)
- Romero-Calcerrada R, Perry GLW (2004) The role of land abandonment in landscape dynamics in the SPA Encinares del río Alberche y Cofio, Central Spain, 1984–1999. *Landsc Urban Plan* 66:217–232. doi:[10.1016/S0169-2046\(03\)00112-9](https://doi.org/10.1016/S0169-2046(03)00112-9)
- Russ JC (1994) *Fractal surfaces*. Plenum Press, New York
- Saura S, Castro S (2007) Scaling functions for landscape pattern metrics derived from remotely sensed data: are their subpixel estimates really accurate? *ISPRS J Photogramm Remote Sens* 62:201–216. doi:[10.1016/j.isprsjprs.2007.03.004](https://doi.org/10.1016/j.isprsjprs.2007.03.004)
- Sugihara G, May RM (1990) Applications of fractals in ecology. *Trends Ecol Evol* 5:79–86. doi:[10.1016/0169-5347\(90\)90235-6](https://doi.org/10.1016/0169-5347(90)90235-6)
- Uuemaa E, Roosaare J, Mander Ü (2005) Scale dependence of landscape metrics and their indicatory value for nutrient and organic matter losses from catchments. *Ecol Indic* 5:350–369. doi:[10.1016/j.ecolind.2005.03.009](https://doi.org/10.1016/j.ecolind.2005.03.009)
- Vicsek T (1989) *Fractal growth phenomena*. World Scientific, Singapore
- Wu J, Jelinski DE, Luck M, Tueller PT (2000a) Multiscale analysis of landscape heterogeneity: scale variance and pattern metrics. *Geogr Inf Sci* 6:6–19
- Wu XB, Thurnow TL, Whisenant SG (2000b) Fragmentation and changes in hydrologic function of tiger bush landscapes, South–West Niger. *J Ecol* 88:790–800. doi:[10.1046/j.1365-2745.2000.00491.x](https://doi.org/10.1046/j.1365-2745.2000.00491.x)
- Zurlini G, Zaccarelli N, Petrosillo I (2006) Indicating retrospective resilience of multi-scale patterns of real habitats in a landscape. *Ecol Indic* 6:184–204. doi:[10.1016/j.ecolind.2005.08.013](https://doi.org/10.1016/j.ecolind.2005.08.013)